

Estimation of Average Rician K-factor in Reverberation Chamber

#Xiaoming Chen¹, Per-Simon Kildal², Jan Carlsson³

^{1,2} Signals and Systems, Chalmers University of Technology

Gothenburg, Sweden, xiaoming.chen@chalmers.se, per-simon.kildal@chalmers.se

³ Electronics Department, SP Technical Research Institute of Sweden
Boras, Sweden, jan.carlsson@sp.se

Abstract

By loading the reverberation chamber (RC) Rician fading can be generated. This paper shows K-factor is reduced by platform stirring. The platform stirring is also used to determine an average K-factor in the chamber, valid for an arbitrary fixed position of the antenna inside the chamber.

Keywords : Reverberation chamber K-factor Mode bandwidth

1. Introduction

Reverberation chamber (RC) is basically a metal cavity with many excited modes that are stirred to create statistical environments with Rayleigh fading. It has been used to measure diversity and capacity performances of multi-port antenna [1]-[4]. RC can also be used to measure total radiated power and total isotropic sensitivity of active mobile phones [5]. Channel sounding in RC was done in [6] to determine the delay spreads and coherence bandwidth affecting such active measurement. RC can also be used to emulate Rician fading environments [7]. In antenna efficiency measurements, the direct coupling or Line-Of-Sight (LOS) component between the transmitting and receiving antenna in the chamber will represent a residual error that degrades measurement accuracy [8]. However, in active measurements, i.e., communication between mobile terminal and base station, Rician fading environments could be desirable in order to emulate realistic suburb or rural multipath environments. As a result, it is important to determine the K-factor in RC. In [7], different methods to control K-factor are studied and presented. While most of the methods are valid only for large directive antennas, loading of the chamber will also work for non-directive small antennas. In the present paper, different loadings in the form of absorbing objects are located in an RC. The RC used for the present measurements is Bluetest High Performance RC with a size of 1.8m×1.7m×1.2m. In Bluetest RC, there are three wall antennas mounted at three orthogonal walls, and used for polarization stirring [9]. The antenna under test (AUT) is placed on a platform, which will rotate during measurements, referred to as platform stirring [9]. Two metal plates are used as mechanical plate stirrers. They can move along corresponding walls either simultaneously, or sequentially, the latter meaning one stepwise after the other in a special sequence. In addition, certain lossy objects are used to control the fading environment. In the present paper we use five loading configurations. The empty RC is denoted *load0*. The head phantom filled with brain equivalent liquid is *load1*. And, *load2*, *load3* and *load4* correspond to the head phantom plus three, six, and nine Polyvinyl Chloride (PVC) cylinders filled with microwave foam absorbers, respectively, in the same way as in [6].

2. K-Factor

Normally, in rich scattering multipath environment, if there is no LOS or direct coupling, the channel response can be assumed to have Rayleigh fading; and if there is a LOS component, the channel response will have Rician fading [10]. The Rician K-factor is for measurements in the RC estimated by [7], [10]

$$K = P_d / P_s \quad (1)$$

$$P_d = |\overline{S_{21}}|^2 \quad ; \quad P_s = |\overline{S_{21} - \overline{S_{21}}}|^2$$

where P_d is the power of the LOS component $\overline{S_{21}}$ of the total transfer function S_{21} , and P_s is the averaged power of the statistical scattering component of S_{21} . The total transfer function S_{21} is most conveniently measured with a vector network analyzer (VNA) between two antennas in the RC. $\overline{S_{21}}$ means complex average of S_{21} over all stirrer position, and $|\overline{S_{21} - \overline{S_{21}}}|^2$ means the average of $|S_{21} - \overline{S_{21}}|^2$ over all stirrer positions. In order to illustrate the K-factor more clearly, the platform is moved to 5 positions spaced by $360\text{deg}/5=72$ deg, and for each platform position each of the two stirrer plates move sequentially to 10 positions, each distributed evenly along the total distance they can move. Thereby, $10 \times 10 = 100$ plate stirrer configurations are created for each platform position. The number of platform positions was limited to 5 in order to reduce measurement time. At each stirrer position and for each of the three wall antennas, a full frequency sweep is performed by the VNA. Therefore, for each frequency there are 1500 samples in total.

Fig. 1 shows plots of the complex channel transfer function S_{21} between the AUT and one of the wall antennas only, at 900 MHz, for two loading configurations. We see that the points representing the channel transfer function as a function of plate stirrer position are more spread for the empty chamber than the loaded one. We also see that for the loaded chamber the channel transfer function generate five distinguishable groups, one for each platform position. This means that each platform position has a different K-factor represented by the center of the complex S_{21} clouds of each platform position. The other loading configurations show the same tendency; the S_{21} clouds separate more and more with increasing loading, but they are not included for brevity. This means that the K-factor for each of the platform position increases with increasing loading. However, the five S_{21} clouds form together a joint cloud with much smaller K-factor, so that platform stirring is a very effective way of removing the effect of the direct coupling and LOS component. Note that in RC unstirred multipath components may appear if the stirrers are not very effective [7]. Such unstirred components are deterministic and show up in the measurements in the same way as a direct coupling or LOS component. Since both unstirred and LOS components have the same effects on the RC performance, we will not discuss them separately in the present paper. Thus, P_d in (1) is the apparent direct coupled power.

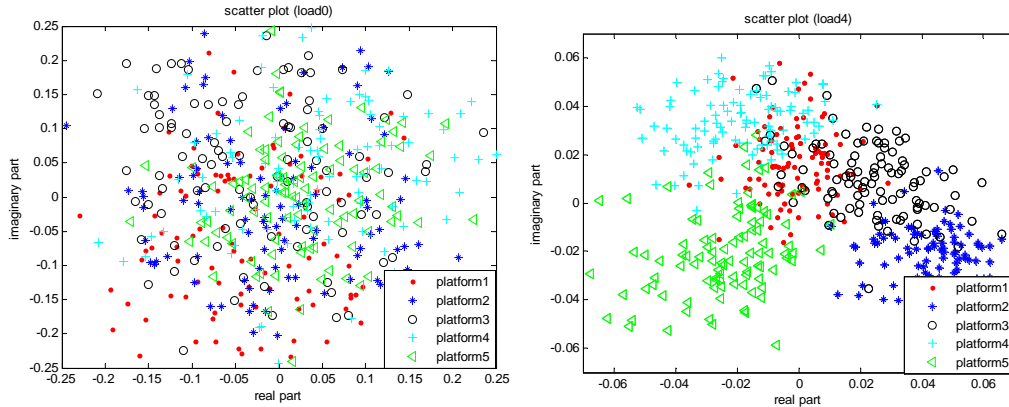


Fig. 1. Stirrer plots of S_{21} for the load0 (left) and load4 (right) configurations, each for 5 platform positions and 100 plate positions per platform position, at 900 MHz.

When the RC is provided with platform and polarization stirring, it is convenient to define an average K-factor in the following way. For each wall antenna and platform position we calculate P_d and P_s and the K-factor by using (1). Thereafter, we obtain the average K-factor, obtained by averaging (or simply summing) P_d and P_s over the five platform positions and three wall antennas, and using

$$K_{av} = \sum P_d / \sum P_s \quad (2)$$

Such calculated average K-factors are shown in Fig. 2 (left). To reduce their statistical variations due to the finite number of stirrer positions, both P_d and P_s have been smoothed over a floating window of 20 MHz before plotted. The average K-factors are slightly decreasing with increasing frequency, in contrast to the K-factors in [7] that increase with frequency. The reason is that the authors of [7] used directive horn antennas as both transmitting and receiving antennas, and their gains are known to increase with frequency, whereas in the present paper, small non-directive antennas are used, and therefore the K-factors obtained here are almost constant with frequency. Fig. 2 (right) shows the K-factor evaluated in the same way, but by using all platform positions directly in equation (1), so that we get the overall K-factor of all the 1500 complex S_{21} samples for each frequency point and loading configuration. We see that the K-factors in Fig. 2 (right) are much lower than in Fig. 2 (left), meaning that the platform and polarization stirring significantly reduce the K-factors. Fig. 3 shows how all the complex S_{21} samples in Fig. 1 look after their direct coupling (complex average) has been removed for each platform position, using

$$S_{21}^{NLOS} = S_{21} - \overline{S_{21}} \quad (3)$$

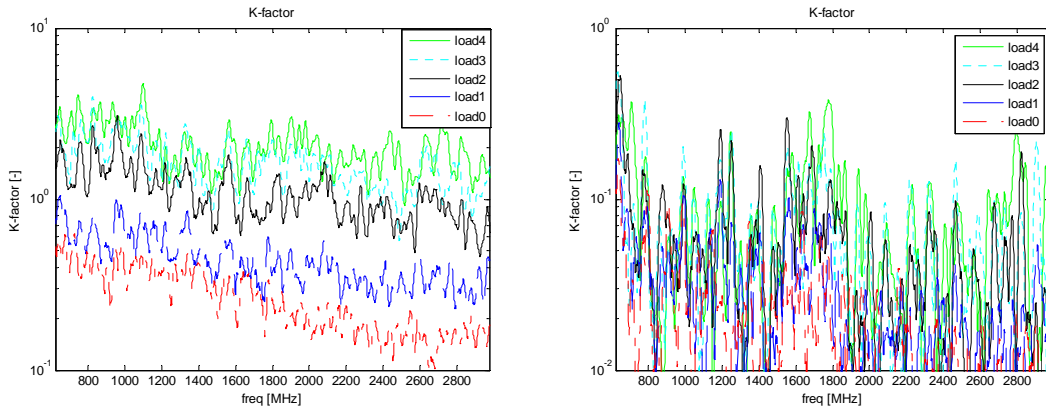


Fig. 2. Average K-factors according to (2) (left). K-factors calculated from all 1500 stirrer positions by using (1) directly (right). All curves are obtained by smoothing both P_d and P_s over 20 MHz, respectively, before evaluating K.

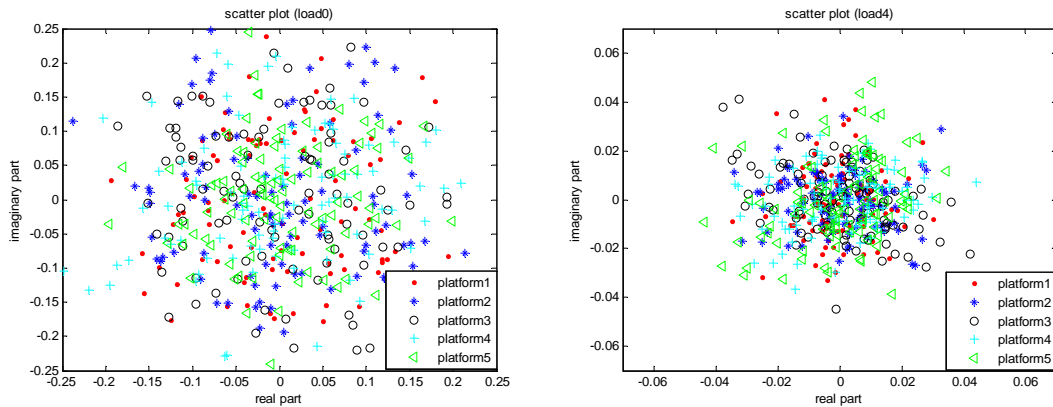


Fig. 3. Stirrer plots of the complex S_{21} in Fig. 2 after removal of the direct coupling in each of the five platform positions, for the load0 (left) and load4 (right) configurations.

3. Conclusion

We have shown that the K-factor in RC almost disappears when platform stirring is applied, because the LOS component (over different platform positions) is randomized. For heavy loading, it is found that the K-factor is reduced approximately inversely proportional to the number of platform

position. If Rician environment with large K-factor is desired, platform stirring cannot be used. We have defined an average characterizing Rician K-factor for reverberation chambers with platform and polarization stirring. This average K-factor is the K-factor valid for non-directive antennas, when platform and polarization stirring is not used, although it is found by averaging the K-factor observed in each platform position.

References

- [1] K. Rosengren and P.-S. Kildal, "Radiation efficiency, correlation, diversity gain and capacity of a six-monopole antenna array for a MIMO system: theory, simulation and measurement in reverberation chamber," *IEE Proc. Microw. Antennas Propag.* Vol. 152, pp. 7-16, 2005. See also Erratum published in August 2006.
- [2] X. Chen, P.-S. Kildal, J. Carlsson, "Fast converging measurement of MRC diversity gain in reverberation chamber using covariance-eigenvalue approach," to be published in *IEICE Transactions on Electronics*, vol.E94-C, no.10, pp.-, Oct. 2011.
- [3] X. Chen, P.-S. Kildal, J. Carlsson, "Simple calculation of ergodic capacity of lossless two-port antenna system using only S-parameters – Comparison with common Z-parameter approach," *IEEE International Symposium on Antennas and Propagation*, Spokane, USA, 3-8 July, 2011.
- [4] X. Chen, P.-S. Kildal, J. Carlsson, J. Yang, "Comparison of Ergodic Capacities from Wideband MIMO Antenna Measurements in Reverberation Chamber and Anechoic Chamber," Accepted for publication in *IEEE Antennas and Wireless Propagation Letters*, 2011.
- [5] C. Orlenius, P.-S. Kildal and G. Poilasne, "Measurement of Total Isotropic Sensitivity and Average Fading Sensitivity of CDMA phones in Reverberation Chamber," *IEEE AP-S Internal Symp.*, Washington D.C., July, 2005.
- [6] X. Chen, P.-S. Kildal, C. Orlenius, J. Carlsson, "Channel sounding of loaded reverberation chamber for Over-the-Air testing of wireless devices - coherence bandwidth and delay spread versus average mode bandwidth", *IEEE Antennas and Wireless Propagation Letters*, vol. 8, pp. 678-681, 2009.
- [7] C. L. Holloway, D. A. Hill, J. M. Ladbury, P. F. Wilson, G. Koepke, and J. Coder, "On the Use of Reverberation Chamber to Simulate a Rician Radio Environment for the Testing of Wireless Devices," *IEEE Trans. on antennas and propagation*, vol. 54, No. 11, pp. 3167-3177, Nov. 2006.
- [8] P.-S. Kildal, S. Lai, and X. Chen, "Direct Coupling as a Residual Error Contribution during OTA Measurements of Wireless Devices in Reverberation Chamber", *IEEE AP-S*, Charleston, USA, June 1-5, 2009.
- [9] P.-S. Kildal and K. Rosengren, "Correlation and capacity of MIMO systems and mutual coupling, radiation efficiency and diversity gain of their antennas: Simulations and measurements in reverberation chamber," *IEEE Communications Magazine*, vol. 42, no. 12, pp. 102-112, Dec. 2004.
- [10] T. S. Rappaport, *Wireless Communications—Principles and Practice*. 2nd edition, Prentice Hall PTR, 2002, pp.196-202.
- [11] D. A. Hill, M. T. Ma, A. R. Ondrejka, B. F. Riddle, M. L. Crawford, and R. T. Johnk, "Aperture Excitation of Electrically Large, Lossy Cavities," *IEEE trans. Electromagn. Compat.*, vol.36, no. 3, pp169-178, Aug. 1994.

Acknowledgments

This work has been supported in part by The Swedish Governmental Agency for Innovation Systems (VINNOVA) within the VINN Excellence Center Chase.